Supplementary Information

Comparative magnetic resonance analysis of three forms of fentanyl

Kamal Wagle[1,2], Adam R. Altenhof[3], Madelyn G. Crotzer[1], Marc A. Alvarez[4], Rami J. Batrice[4], Robert F. Williams[4], Aaron M. Tondreau[5], Ann E. Mattsson[1], Harris E. Mason[5], Daniel A. Rehn[*1], Michael W. Malone[†3]

[1]Computational Physics Division, Los Alamos National Laboratory, Los Alamos, NM 87545, USA
[2]Center for Nonlinear Studies, Los Alamos National Laboratory, Los Alamos, NM 87545, USA
[3]Materials Physics and Applications Division, Los Alamos National Laboratory, Los Alamos, NM 87545, USA
[4]Biochemistry and Biotechnology, Los Alamos National Laboratory, Los Alamos, NM 87545, USA
[5]Chemistry Division, Los Alamos National Laboratory, Los Alamos, NM 87545, USA

Contents

[*]rehnd@lanl.gov
[†]mwmalone@lanl.gov

1 Geometry

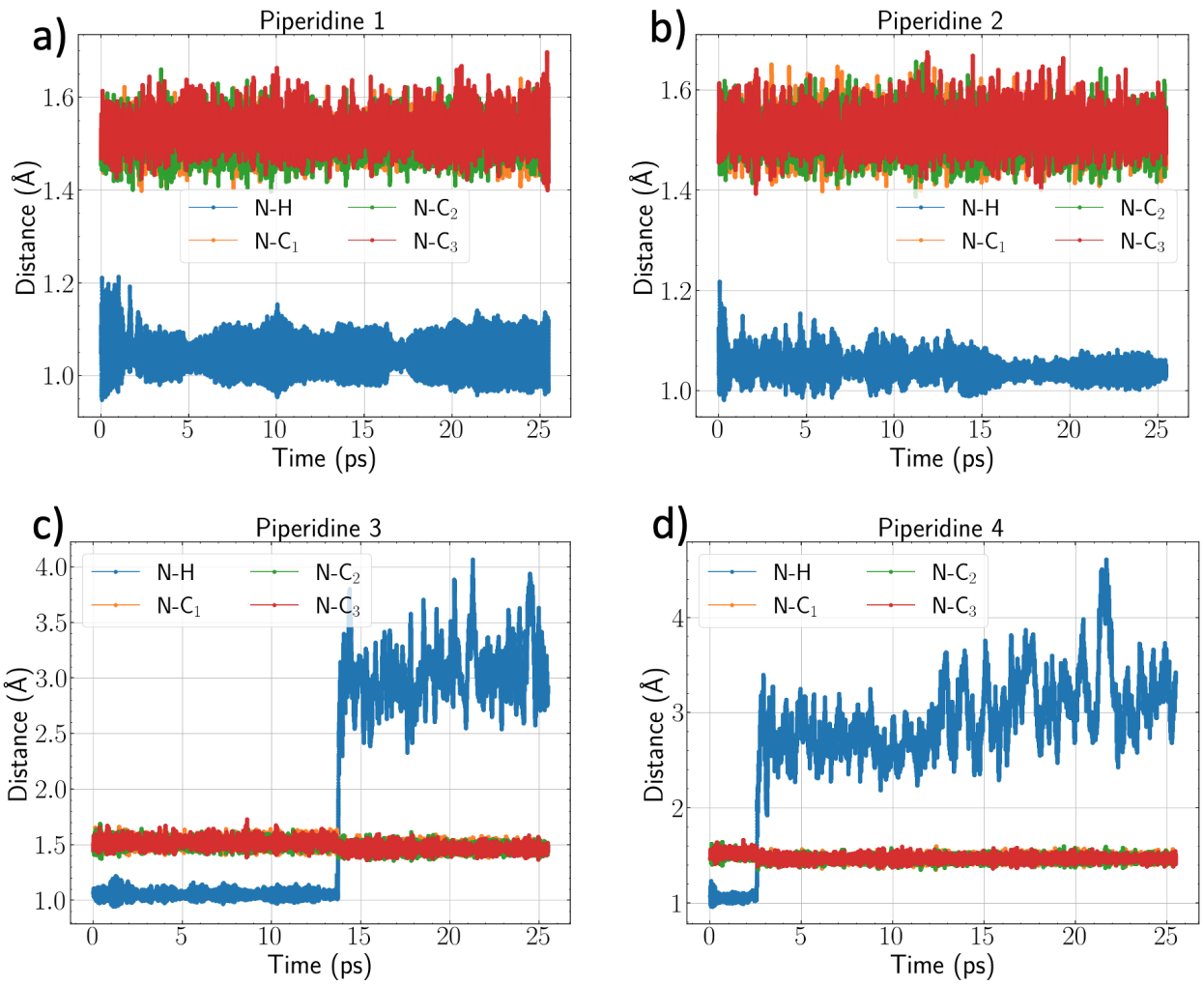

Figure S1: The four subplots represents how four nearest neighbors of each of four hydrogen-added piperidines in fentanyl-freebase change during DFT-MD.

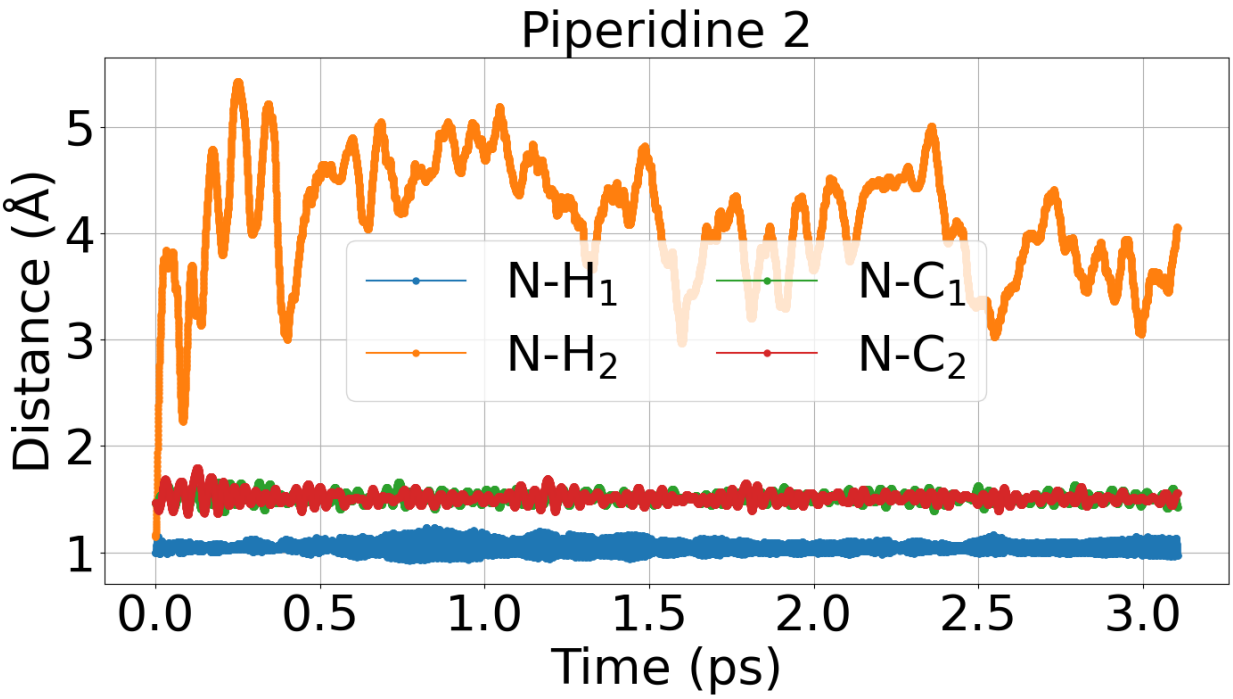

Figure S2: The figure represents how four nearest neighbors of H-added P_2 piperidine site of fentanyl-freebase is stablized with an additional H_2O molecule change during DFT-MD.

Table S1: Structural parameters such as lattice parameters, space group, volume, and atoms of each type present in unitcell of three fentanyl types; free-base, citrate, and hydrochloride.

Parameter/Type	fentanyl freebase	fentanyl citrate	Fentanyl HCl
a($\AA$)	5.69263	8.963	10.7319
b($\AA$)	25.1851	11.2533	27.228
c($\AA$)	13.8608	14.874	7.0662
$\alpha(^\circ)$	90	109.411	90
$\beta(^\circ)$	104.2037	96.728	95.843
$\gamma(^\circ)$	90	107.486	90
Space group	$P2_1/c$ (# 14) Monoclinic	$P\bar{1}$ (# 2) Triclinic	C_c (# 9) Monoclinic
Volume ($\AA^3$)	1926.4652	1309.7207	2054.0739
N	8	4	8
O	4	16	4
C	88	56	88
H	113	72	116
Cl	0	0	4
Total atoms	212	148	220

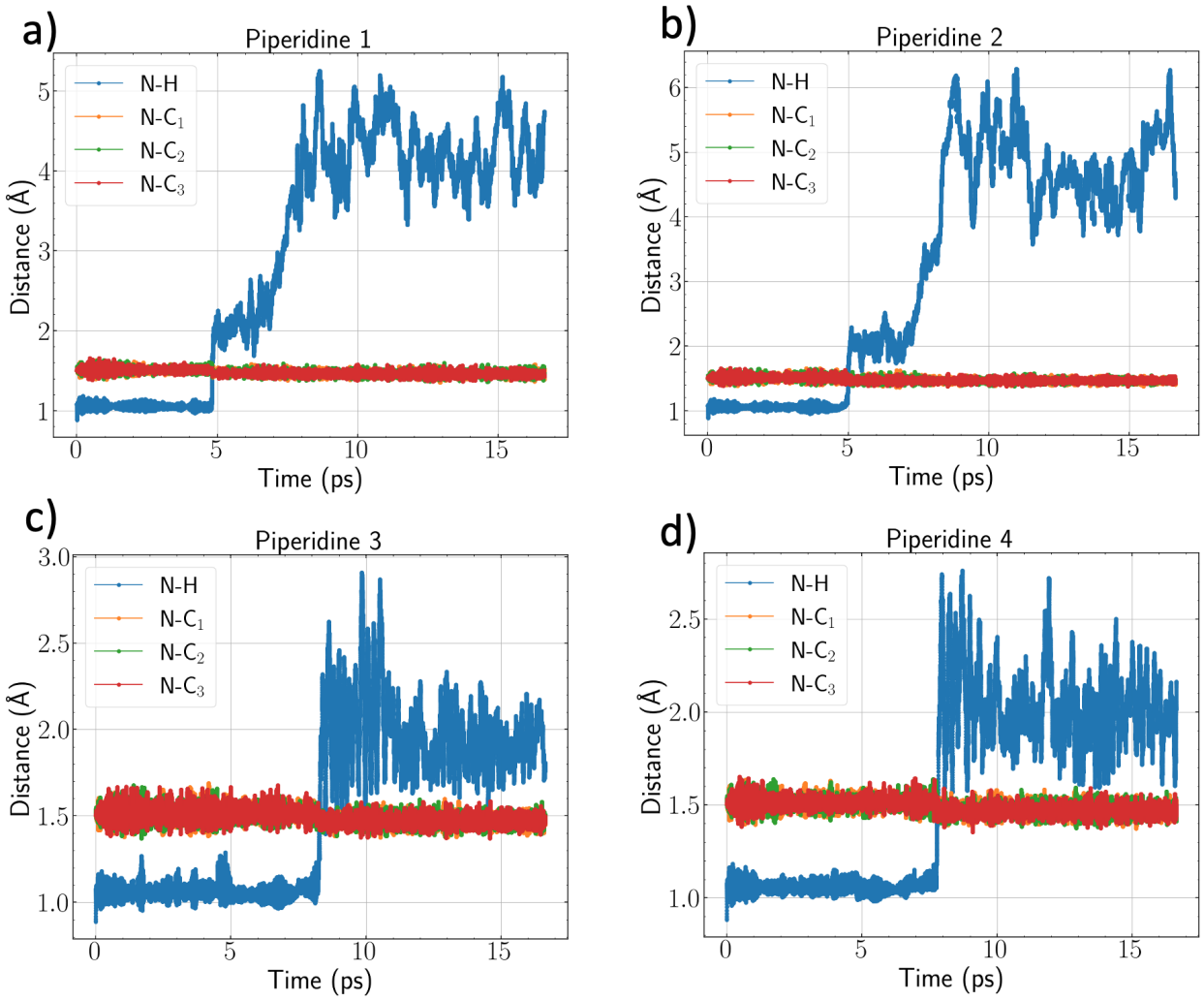

Figure S3: The four subplots represents how four nearest neighbors of each of four Cl-removed piperidines in fentanyl-HCl change during DFT-MD.

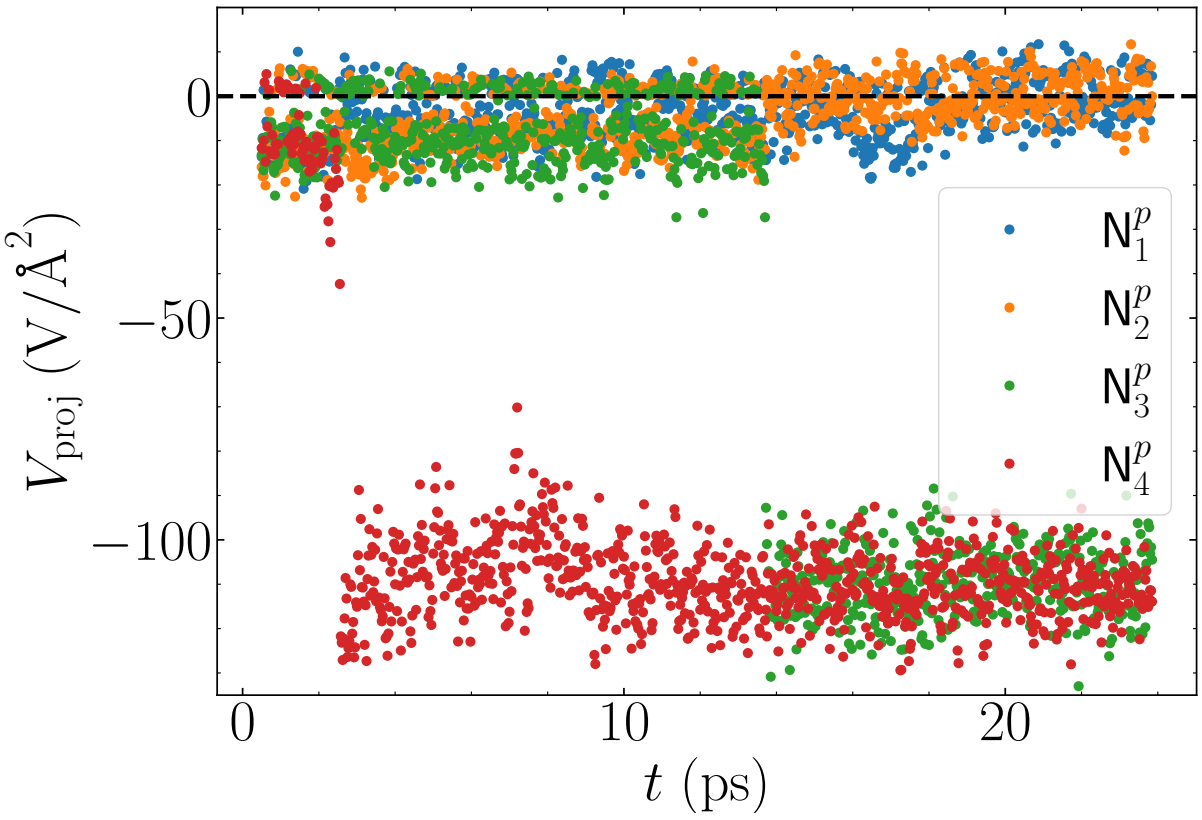

Figure S4: V_{zz} of fentanyl freebase with one hydrogen atom attached to each of the piperidine nitrogen sites.

2 Phonon densities of states

To ensure convergence of vibrational properties from the MD trajectory, we calculate the phonon density of states (PDOS) of individual atoms in each of the three fentanyl structures. The convergence was assured with the help of PDOS obtained from larger cell size ($2 \times 1 \times 1$) from representative fentanyl freebase. All the PDOS spectra shown in Fig. S5 are calculated using the velocity autocorrelation (VAC) of the MD trajectories. For a Representative structure (fentanyl freebase), this was also in close agreement with a static phonon obtained using the finite displacement method as implemented in the Phonopy. [1, 2] The agreement in the PDOS spectrum of common atom types across fentanyl types as shown in Fig. S5 is also reflective of the fact that MD trajectories are sufficiently accurate.

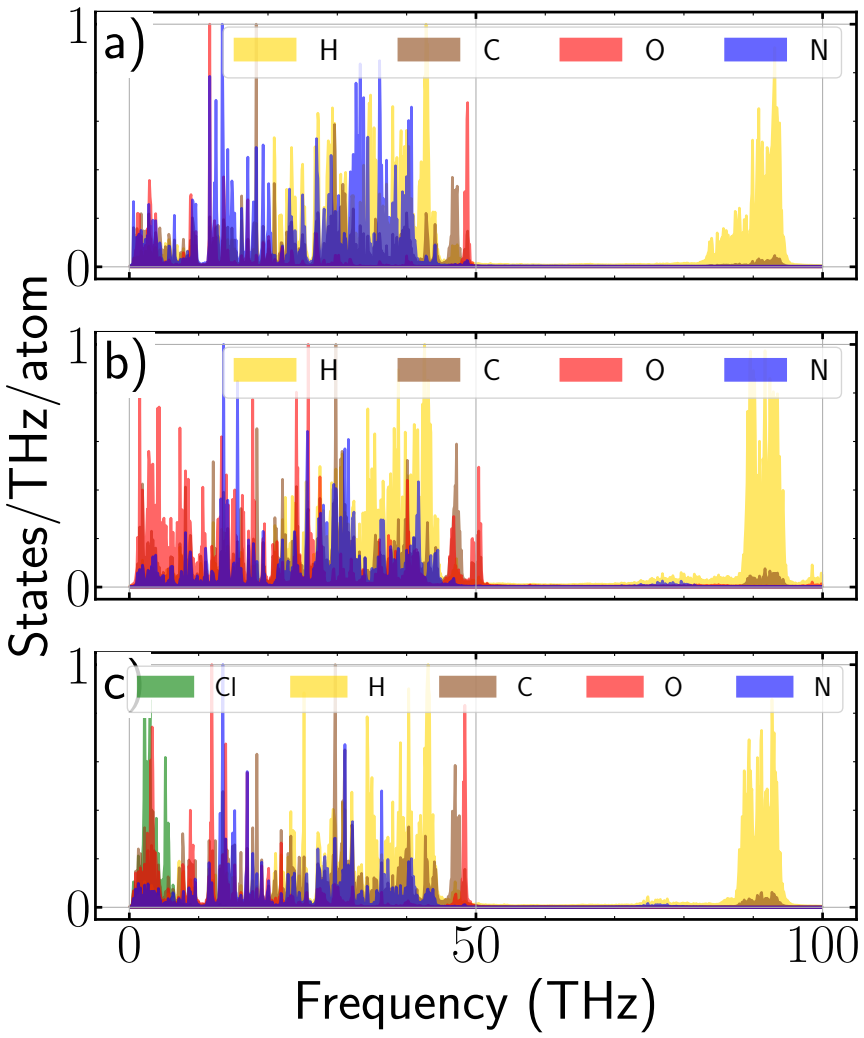

Figure S5: Normalized phonon density of states for each atom in a) fentanyl freebase, b) fentanyl citrate, and c) fentanyl HCl.

3 Projection scheme for EFGs

To study the effect of the dynamical motion of atoms on the EFG parameters, we use a projection scheme that we developed in Ref. [3]. Here we briefly review the method. We define the eigenvalues of the static structure as V_{ii} $(i = 1, 2, 3 = x, y, z)$. The normalized eigenvectors associated with V_{ii} are labeled $\hat{e}_i$. This allows us to use a compact notation $\boldsymbol{V}_{ii} = V_{ii}\hat{e}_i$ to discuss the eigenvalue along the direction of its associated eigenvector in the lattice reference frame, i.e., $\boldsymbol{V}_{xx} = V_{xx}\hat{e}_1$, $\boldsymbol{V}_{yy} = V_{yy}\hat{e}_2$, $\boldsymbol{V}_{zz} = V_{zz}\hat{e}_3$. Similarly, we label the eigenvalues of the instantaneous snapshots from the MD trajectory as V'_{ii}, and these are associated with normalized eigenvectors in the lattice frame $\hat{e}'_i$ so that we can define vectors $\boldsymbol{V}'_{ii} = V'_{ii}\hat{e}'_i$. We also note that the signs of the eigenvectors $\hat{e}_i$ and $\hat{e}'_i$ are arbitrary. In order to maintain consistency in presenting our results, we choose the sign of the eigenvectors such that $\hat{e}'_i \cdot \hat{e}_i > 0$, with $\hat{e}_i$ being a fixed value, as it comes from the static calculation.

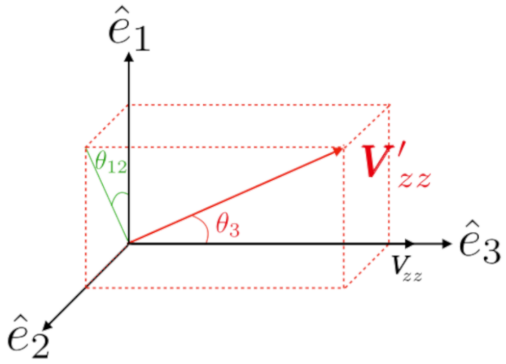

Figure S6: Schematic of the direction of dynamic $\boldsymbol{V}'_{zz}$ and static $\boldsymbol{V}_{zz}$, angle θ_3 between $\boldsymbol{V}'_{zz}$ and $\boldsymbol{V}_{zz}$, and angle θ_{12} in the plane perpendicular to static $\boldsymbol{V}_{zz}$. Normalized eigenvectors in the static frame are labeled $\hat{e}_i$ here.

Using this notation, we investigate how the dynamical EFGs $\boldsymbol{V}'_{zz}$ change relative to the static $\boldsymbol{V}_{zz}$ throughout the MD simulation. We considered variation in three quantities shown in Fig. S6: the angle between the directions of the dynamic $\boldsymbol{V}'_{zz}$ (or $\hat{e}'_3$) and static $\boldsymbol{V}_{zz}$ (or $\hat{e}_3$) denoted by θ_3, the variation in the magnitude of projection of $\boldsymbol{V}'_{zz}$ onto $\hat{e}_3$ denoted by V_{proj}, and the angle θ_{12} of $\hat{e}'_3$ projected onto the $\hat{e}_1$–$\hat{e}_2$ plane. These values are calculated in the following way,

$$\theta_3 = \arccos\left(\hat{e}'_3 \cdot \hat{e}_3\right) \tag{1}$$

$$V_{\text{proj}} = V'_{zz}\cos\theta_3 \tag{2}$$

$$\theta_{12} = \arccos\frac{\hat{e}'_3 \cdot \hat{e}_1}{\sqrt{(\hat{e}'_3 \cdot \hat{e}_1)^2 + (\hat{e}'_3 \cdot \hat{e}_2)^2}} \tag{3}$$

References

[1] Atsushi Togo. First-Principles Phonon Calculations with Phonopy and Phono3py. *J. Phys. Soc. Jpn.*, 92(1):012001, 2023.

[2] Togo, Atsushi and Chaput, Laurent and Tadano, Terumasa and Tanaka, Isao. Implementation strategies in phonopy and phono3py. *J. Phys.: Condens.Matter*, 35(35):353001, 2023.

[3] Kamal Wagle, Daniel A Rehn, Ann E Mattsson, Harris E Mason, and Michael W Malone. Effect of dynamical motion in ab initio calculations of solid-state nuclear magnetic and nuclear quadrupole resonance spectra. *Chemistry of Materials*, 2024.